Nearest-neighbor exchange constant and Mn distribution in $Zn_{1-x}Mn_xTe$ from high-field magnetization step and low-field susceptibility

Y. Shapira, S. Foner, P. Becla, and D. N. Domingues
Francis Bitter National Magnet Laboratory, Massachusetts Institute of Technology, Cambridge, Massachusetts 02139

M. J. Naughton and J. S. Brooks
Department of Physics, Boston University, Boston, Massachusetts 02215
(Received 5 August 1985)

Magnetization data in fields up to 210 kOe were obtained on $Zn_{1-x}Mn_xTe$ samples with $x=0.031$ and 0.040. At $T\cong 1.4$ K, a magnetization step was observed near 150 kOe. This step is attributed to a level crossing for pairs of nearest-neighbor (NN) Mn spins. The magnetic field at the center of the step gives $J/k_B=-10.0\pm 0.8$ K for the NN exchange constant. This value is slightly higher than that obtained from inelastic neutron scattering. The magnitude of the magnetization step agrees with calculations which assume a random Mn distribution. The technical saturation value for the magnetization at low temperatures also agrees with calculations which assume a random Mn distribution. Low-field susceptibility data, taken at $4\leq T\leq 350$ K, lead to Curie constants which agree with those calculated with $S=\frac{5}{2}$ and $g=2$ for each Mn ion. Assuming NN interactions only, and a random Mn distribution, the Curie-Weiss temperatures give $J/k_B\cong -12$ K. A detailed theoretical discussion of the NN cluster model, as it applies to the magnetization curve of a dilute magnetic semiconductor at low T, is given. Many of the theoretical results also should apply to a larger class of dilute magnetic materials.

I. INTRODUCTION

The most extensively studied dilute magnetic semiconductors (DMS's) are II-VI compounds, such as CdTe or ZnTe, in which a fraction x of the cations has been replaced by Mn.[1] The magnetic properties of these materials have been studied for at least two decades.[2] These studies are reviewed in Refs. 3 and 4. Two basic questions were controversial until recently: (1) Is the Mn distribution over the cation sites random? (2) What is the magnitude of the exchange constant J between nearest-neighbor (NN) Mn spins? Answers to these questions were recently obtained from analyses of magnetization and optical reflectivity data in terms of a simple NN cluster model.[5–7] It was concluded that in the materials investigated the Mn distribution was random, and $J/k_B\sim -10$ K, where k_B is the Boltzmann constant. The determination of J was based on the new phenomenon of magnetization steps at high magnetic fields and low temperatures.

In this paper we present magnetization and susceptibility data for two samples of $Zn_{1-x}Mn_xTe$, with $x=0.031$ and 0.040. The magnetization data were taken at temperatures $1.3\leq T\leq 1.5$ K in magnetic fields H up to 210 kOe. The susceptibility data were taken at low H for temperatures $4\leq T\leq 350$ K. A detailed analysis of the data indicates that also in these samples the Mn distribution is random, and $J/k_B\cong -10$ K. In addition, it is shown that the low-temperature magnetization of the samples in fields near 100 kOe is given quantitatively by the NN cluster model of Ref. 5. A comparison with two other recent studies[8,9] of the magnetic properties of $Zn_{1-x}Mn_xTe$ is also given.

Before presenting the data and their analysis, we discuss the NN cluster model which is outlined in Ref. 5, and the theory for the susceptibility at high temperatures. Although the theoretical discussion focuses specifically on II-VI DMS's, many of the results apply to a larger class of dilute magnetic materials for which the assumptions of the model hold.

II. THEORY

A. Assumptions

Each Mn ion is assumed to have a spin $S=\frac{5}{2}$ and a g factor $g=2$. The assumption $g=2$ is supported by paramagnetic resonance[4,10–13] and Raman[14] experiments on Mn in various II-VI semiconductors (including ZnTe), which indicate that the deviation of g from 2.00 is less than 1%. The assumption $S=\frac{5}{2}$ is supported by experimental results for the Curie constant C in the II-VI DMS's.[4,5,13,15,16] In particular, the Curie constants of the two $Zn_{1-x}Mn_xTe$ samples which were measured in the present work agree closely with values calculated assuming $S=\frac{5}{2}$ and $g=2$.[17]

The energy of the Mn spins in a DMS is affected by several interactions. These include (1) the d-d exchange interaction between the Mn spins, (2) The Zeeman energy, if a magnetic field **H** is present, (3) dipole-dipole interactions between the Mn spins, (4) interactions with crystal fields, and (5) the s-d interaction between the Mn spins and the spins of electrons (holes) near the band edges. In what follows we assume that only the d-d exchange interaction and the Zeeman interaction are important; all other interactions will be ignored. The reasons for making the last assumption are the following. First, we will

be concerned only with relatively pure samples (with low carrier concentrations), for which the magnetization is not significantly affected by the *s-d* interaction. Second, the theoretical discussion in this section focuses on only two regimes of temperature and magnetic field: (1) $H \gtrsim 100$ kOe and $T \lesssim 2$ K, and (2) $T > 100$ K and $g\mu_B H < k_B T$, where μ_B is the Bohr magneton. In these two regimes the relatively weak dipole-dipole and crystal-field interactions[4,10–12] are not expected to change the magnetization significantly. We note, however, that these weak interactions can become important in the regime of low temperatures and low magnetic fields ($T \lesssim 1$ K and $H \lesssim 10$ kOe) which will not be considered in this paper.

The dominant *d-d* exchange interaction in the II-VI DMS's is the antiferromagnetic interaction between NN Mn spins.[2,18–23] For two NN spins, $\mathbf{S}_i$ and $\mathbf{S}_j$, the exchange Hamiltonian can be written as

$$\mathscr{H}_{\text{ex}} = -2J\mathbf{S}_i \cdot \mathbf{S}_j \ , \tag{1}$$

where J is the NN exchange constant, which is negative for an antiferromagnetic interaction. Recent experiments[4–7,19,20,22] and calculations,[23] as well as some early data,[18] indicate that the values of J/k_B in II-VI DMS's are equal to -10 K within a factor of 2 or so. The much smaller values of J which were deduced by some workers[3,24,25] are now believed to be incorrect.[5]

The available information concerning the next-nearest-neighbor (NNN) exchange constant J' in II-VI DMS's suggests that it is 1 or 2 orders of magnitude smaller than J, and that J' too is negative (antiferromagnetic).[2,18–23] We are unaware of any direct information concerning J' in $Zn_{1-x}Mn_xTe$, but we expect that in this material also $|J'| \ll |J|$. In the theoretical discussion which follows, we assume that $|J'/J| \lesssim 0.1$, or $|J'/k_B| \lesssim 1$ K for $Zn_{1-x}Mn_xTe$. The behavior of the magnetization will then be discussed in two stages. First, the NNN interaction (and interactions between more distant neighbors) will be ignored. Later, the effects of a NNN interaction with $|J'/k_B| \lesssim 1$ K will be estimated. It will turn out that these effects are small in the two regimes of interest: (i) when $H \gtrsim 100$ kOe and $T \lesssim 2$ K, and (ii) when $T > 100$ K. It must be emphasized, however, that outside these two regimes the relatively weak NNN interaction can have a major influence on the magnetization. Specifically, if neither the thermal energy $k_B T$ nor the Zeeman energy $g\mu_B H$ is larger than the NNN energy $2|J'|S^2$, then the NNN interaction can be important.[2]

There is now strong evidence that the distribution of Mn ions in typical crystals of II-VI DMS's is random.[5] Such a random Mn distribution will be assumed in some parts of the theoretical discussion. In each of these cases the assumption will be stated explicitly. Results which are independent of this assumption will be pointed out.

B. NN cluster model for the magnetization at high H and low T

1. The model

In the NN cluster model all exchange interactions other than those between NN spins are ignored. The basic idea of the model[24] is that the magnetization M of a dilute magnetic alloy is the sum of the magnetizations of independent clusters of NN spins. There are different types of clusters: The smallest cluster, called a single, consists of an isolated Mn spin. Next is a cluster which consists of two spins, called a pair. Clusters which consist of three spins are of two types, (1) closed triangles (CT's), in which all three spins are NN's of each other, and (2) open triangles (OT's), in which the first and second spins are NN's, as are the second and third spins, but the first and third spins are not NN's. Clusters which contain more than three spins are also present in a dilute magnetic alloy. However, if the concentration of the magnetic ions is low, and if the distribution of these ions is random, then the probabilities of occurrence of these larger clusters are small. For example, in the zinc-blende structure of $Zn_{1-x}Mn_xTe$, 97% of the spins are in clusters of three spins or less for $x = 0.03$, and 94% for $x = 0.04$. These percentages should be applicable to the samples which were studied in the present work. Therefore, to describe the magnetization at high H and low T we will use the approximation in which clusters with more than three spins are ignored. This approximation turns out to be quite accurate for $x < 0.05$, and is not unreasonable even for x as large as 0.1, for presently available dc magnetic fields.

It will be useful to use an index c to describe the cluster type. Thus, $c = 1$ for a single, $c = 2$ for a pair, $c = 3$ for an OT, and $c = 4$ for a CT. The number of spins in a cluster will be designated by n_c.

2. Magnetization process at low T

In this section we discuss *qualitatively* the magnetization curve of a DMS with low x at temperatures $T < 2$ K $\ll 2|J|/k_B$. The discussion is based on the NN cluster model, with clusters containing no more than three spins. Quantitative predictions are summarized later.

A schematic of the expected magnetization curve at low T is shown in Fig. 1. The curve can be divided into two parts: (1) The low-field part (LFP), $0 < g\mu_B H \lesssim 2|J| - 2k_B T$, and (2) the high-field part (HFP), $g\mu_B H \gtrsim 2|J| - 2k_B T$. For the typical values $J/k_B = -10$ K and $T = 1.5$ K, the LFP extends up to approximately 127 kOe. In the LFP the magnetization M increases smoothly with H at a rate which decreases with increasing H. When the top of the LFP is reached, M is nearly independent of H. In the HFP the magnetization exhibits a series of steps. With the presently available dc magnetic fields of up to about 300 kOe, only the first one or two of these steps are expected to be observed.

The magnetization curve in Fig. 1 is a consequence of the energy-level schemes of the clusters. The energy levels for clusters with less than four spins are given in Ref. 24. They have the following properties. At $H = 0$ each cluster has a ground state and a series of excited states, except for singles, which have no excited states. The first excited state is separated from the ground state by an energy $b_c|J|$, where b_c is an integer which depends on the cluster type c. For a pair, $b_2 = 2$. For the two types of triplets, b_c is larger. The total spin S_T is a good quantum

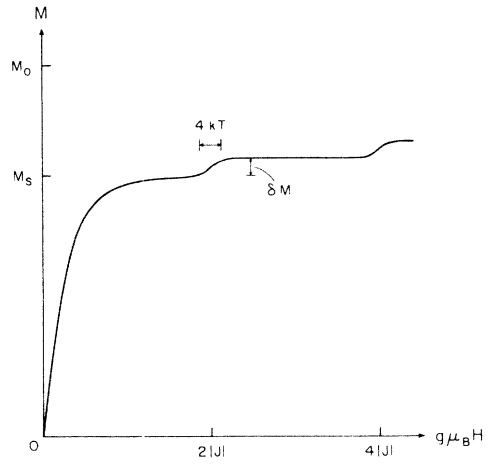

FIG. 1. Sketch of the predicted magnetization curve at low temperatures for a dilute magnetic semiconductor with a low x. Here, M is the magnetization, H is the magnetic field, M_s is the technical saturation value, M_0 is the true saturation value, and J is the NN exchange constant.

number for all energy levels. States with $S_T \neq 0$ are degenerate at $H=0$, but undergo a Zeeman splitting when a magnetic field is applied. States which arise from the Zeeman splitting of a degenerate state will be said to originate from that state. The value of S_T for the zero-field ground state of a cluster of type c will be designated by $S_T(g,c)$. For a single, $S_T(g,1)=\frac{5}{2}$. For all other clusters, $S_T(g,c)<\frac{5}{2}n_c$, i.e., the Mn spins in the zero-field ground state are not parallel to each other.

Consider the LFP of the magnetization curve when $k_BT \ll 2|J|$. It can be shown that in this field range the magnetization of a cluster is solely due to states which originate from the zero-field ground state of the cluster.[5] Physically, states which originate from the zero-field excited states are not populated at these low fields. The magnetization of a cluster in the LFP is therefore equal to that of an isolated effective spin of magnitude $S_T(g,c)$. The LFP of the magnetization curve corresponds to the H-induced alignment of these effective spins for all the clusters. Near the top of the LFP, the magnetization of each effective spin is nearly saturated because $g\mu_B H \gg k_BT$.

We now turn to the magnetization steps in the HFP. Consider a cluster other than a single. At $H=0$ some of the excited states have a total spin S_T which is larger than $S_T(g,c)$. The Zeeman splittings of such states are therefore larger than that of the zero-field ground state. At a sufficiently high field, one of the energy levels which arises from the Zeeman splitting of an excited state will cross the lowest level which originates from the zero-field ground state. This leads to a new ground state with a larger spin component S_T^z along **H**. Thus, the energy-level crossing results in an increase in M. At $T=0$ this increase is sharp, i.e., an abrupt magnetization step occurs. At finite T the step will be thermally broadened, with a width ΔH of about $4k_BT/g\mu_B$.

When the magnetic field is increased further, additional level crossings take place. Each level crossing is associated with an increase of S_T^z and results in a magnetization step. The series of magnetization steps ends when S_T^z assumes the largest possible value for the cluster, which corresponds to a parallel alignment of all the spins in the cluster along **H**. The maximum S_T^z is equal to $\frac{5}{2}n_c$.

Detailed considerations[5] show that the first magnetization step arises from a level crossing for pairs. It occurs at a field H_1 which is given by

$$g\mu_B H_1 = 2|J| \ . \tag{2}$$

The magnetization steps due to the pairs will be discussed in detail later. The magnetization steps which arise from level crossings for CT's and OT's are not easily observed, either because they occur above the available dc field range (about 300 kOe), or because the magnitudes of the steps are very small.[5] Also, singles do not give rise to magnetization steps because there are no excited states at $H=0$. Thus, in most practical situations only the magnetization steps due to NN pairs are important.

3. *Technical saturation of the magnetization at low T*

In this section we discuss the top of the LFP of the magnetization curve. In nearly all II-VI dilute magnetic semiconductors this top lies above 100 kOe. The only known exception is $Cd_{1-x}Mn_xTe$, for which 100 kOe is on the boundary between the LFP and the HFP of the magnetization curve.[7]

Experimental data for many DMS's with low x indicate that the magnetization $M_{\rm LFP}$ in the LFP is well described by the phenomenological equation[26]

$$M_{\rm LFP} = M_s B_{5/2}[5\mu_B H/k_B(T+T_0)] \ , \tag{3}$$

where $B_{5/2}$ is a Brillouin function for spin $S=\frac{5}{2}$, and M_s and T_0 are phenomenological parameters which are nearly temperature independent at low T. For $x<0.1$ and $T<2$ K the magnetization near the top of the LFP is usually nearly H independent, and is close to M_s.[27] We define M_s as the technical saturation value for the magnetization. This M_s should be clearly distinguished from the true saturation value M_0 in the limit $H \to \infty$.

To derive an expression for M_s we use the NN cluster model, restricted to $n_c \leq 3$. Near the top of the LFP the magnetization of each cluster corresponds to the full alignment of an effective spin of magnitude $S_T(g,c)$. Thus, the magnetic moment which each cluster contributes to M_s is $2S_T(g,c)\mu_B$. The contribution of the same cluster to M_0 is equal to $5n_c\mu_B$. For pairs and triplets $2S_T(g,c)<5n_c$, so that $M_s<M_0$.

Let P_c be the probability that a spin is in a cluster of type c, and let

$$R_c = 2S_T(g,c)/5n_c \ . \tag{4}$$

It then follows that

$$M_s/M_0 = \sum_c P_c R_c \ , \tag{5}$$

where, in the present approximation, the sum runs from $c=1$ to $c=4$. In Ref. 5 it has been shown that

$$R_1=1, \quad R_2=0, \quad R_3=\tfrac{1}{3}, \quad R_4=\tfrac{1}{15} \ , \tag{6}$$

where, as before, the subscripts 1,2,3,4 refer to singles, pairs, OT's, and CT's, respectively. Equations (5) and (6) give

$$M_s/M_0=P_1+P_3/3+P_4/15 . \quad (7)$$

Note that the pairs do not contribute to M_s, because $S_T=0$ for the zero-field ground state of a pair.[24]

Equations (5) and (7) indicate that the ratio M_s/M_0 is related directly to the probabilities P_c. In Ref. 5 it was shown that good agreement with data in a number of DMS's is obtained if these probabilities are calculated on the assumption that the Mn ions are randomly distributed over the cation sites. The probabilities P_1-P_4 based on this assumption were originally derived by Behringer,[28] and they are also quoted in a number of other papers.[5,24,29]

The contribution of clusters with $n_c \geq 4$ to M_s/M_0 is neglected in Eq. (7). The data in Ref. 5 suggest that for $x<0.1$ this contribution can be included by adding an empirical correction term to this equation. With this added term,

$$M_s/M_0=(P_1+P_3/3+P_4/15) +[(1-P_1-P_2-P_3-P_4)/5] . \quad (8)$$

The empirical correction term which was just added to Eq. (7) amounts to an assignment of an average effective value $\overline{R}_c=\frac{1}{5}$ to all clusters with $n_c \geq 4$. Such a value for $\overline{R}_c$ is not unreasonable because, for most large clusters of antiferromagnetically coupled spins, R_c should be only a small fraction of unity. For the samples used in the present work the difference between Eqs. (7) and (8) is quite small, i.e., 2% for $x=0.040$ and 1% for $x=0.031$.

Equation (7) also neglects the NNN interaction. The effect of this interaction on M_s/M_0 can be estimated by considering not only NN clusters but also clusters which consist of NNN spins, and mixed clusters of NN's and NNN's. An analysis along these lines was made for the Mn concentrations of the two samples which were used in the present work. A random Mn distribution and $|J'/k_B|<1$ K were assumed. The probabilities for the various types of clusters were taken from Ref. 29. The results gave an estimated upper limit of 5% for the change in M_s/M_0 due to the NNN interaction in these samples. The actual change in M_s/M_0 is expected to be only a fraction of this upper limit.

4. *Magnetization steps due to level crossings of pairs*

The energy-level scheme of a pair[24,30] indicates that at $H=0$ the ground state has $S_T=0$, and the excited states (in order of increasing energy) have $S_T=1,2,3,4,5$. By considering the energy-level crossings[5-7] it was concluded that five magnetization steps will occur at high H and low T. The fields H_r at the centers of the steps are given by

$$g\mu_B H_r=2|J|r , \quad (9)$$

where $r=1,2,3,4,5$. Each step corresponds to an increase of one unit in magnitude of the spin component S_T^z along **H**. Therefore, all the magnetization steps are equal in magnitude. The contribution of the pairs to the true saturation magnetization, as $H\rightarrow\infty$, is P_2M_0. Thus, each of the magnetization steps has a magnitude

$$\delta M=P_2M_0/5 . \quad (10)$$

Two types of information can be obtained directly from observations of the magnetization steps: (1) From any of the fields H_r one can calculate J using Eq. (9). This determination of J does not depend on the assumption of a random Mn distribution. (2) From the observed magnitude of δM and Eq. (10) one obtains the actual probability P_2 that a spin is in a pair.[31] Here it is necessary to know x so that M_0 can be calculated. The experimental result for P_2 can be compared with the probability P_2 which is derived from a random Mn distribution. For the zinc-blende structure of $Zn_{1-x}Mn_xTe$ the latter P_2 is given by[28]

$$P_2(\text{random})=12x(1-x)^{18} . \quad (11)$$

If the width of each step is solely due to thermal broadening, and if $4k_BT \ll 2|J|$, then the steps will be well separated. The magnetization step which is centered at H_r is then described by[6,7]

$$M_r=\frac{\delta M}{1+\exp[g\mu_B(H_r-H)/k_BT]} , \quad (12)$$

where δM is given by Eq. (10).

The NNN interaction, which was neglected thus far, leads to an additional broadening of the magnetization steps and to small shifts in the fields H_r. Some of the NN pairs are coupled to one or more spins which are NNN's. For these pairs, a correction of order $|J'|$ should be added to the right-hand side (rhs) of Eqs. (2) and (9).[32] Since this correction applies only to some of the NN pairs but not to others, it will broaden the step.[33] There also will be a shift of the weighted average of H_r.

Assuming a random distribution of Mn, the probability that a NN pair has no NNN is[29]

$$P=(1-x)^8 , \quad (13)$$

where a zinc-blende structure (with a fcc lattice for the cations) is assumed. For the values of x in the present work, 0.031 and 0.040, this gives 78% and 72% of NN pairs which have no NNN, respectively. Of the remaining pairs, the great majority have only one NNN.[29] The energy-level scheme for a NN pair with only one NNN is known.[34] Assuming that

$$|J'/k_B|<1 \text{ K}=0.1|J/k_B| ,$$

we then estimate that the weighted average of H_1 will differ from that given by Eq. (2) by less than 3% for $x=0.031$ and by less than 4% for $x=0.040$. In addition, at the temperatures of the present experiments (about 1.4 K), the dominant contribution to the width of the first magnetization step should be due to thermal broadening.

C. High-temperature susceptibility

The low-field susceptibility χ of a DMS contains two contributions,

$$\chi=\chi_{\mathrm{Mn}}+\chi_d \ , \tag{14}$$

where χ_{Mn} is the low-field susceptibility due to the Mn spins and χ_d is the diamagnetic susceptibility of the lattice. In the limit of high temperatures, χ_{Mn} obeys the Curie-Weiss law

$$\chi_{\mathrm{Mn}}=C/(T-\Theta) \ , \tag{15}$$

where C is the Curie constant,

$$C=xNg^2\mu_B^2S(S+1)/3k_B \ , \tag{16}$$

N is the total number of cations (magnetic and nonmagnetic), and Θ is the Curie-Weiss temperature. Assuming a random Mn distribution, and exchange interactions between NN's only, Θ is given by[35,36]

$$\Theta=2zxJS(S+1)/3k_B \ , \tag{17}$$

where z is the number of NN cations. For the zinc-blende structure, $z=12$.

If exchange interactions other than between NN's are also included, the expression for Θ (under the assumption of a random Mn distribution) takes the form[16]

$$\Theta=[2xS(S+1)/3k_B]\sum_i z_iJ_i \ , \tag{18}$$

where J_i is the exchange constant between a central Mn spin and another Mn spin which is on the ith coordination sphere, and z_i is the number of cations on this sphere. In the present case, $J_1=J$, $J_2=J'$, $z_1=z=12$, and $z_2=6$. Clearly, the contribution of J' to Θ is small if $|J'/J|<0.1$.

Departures from a random Mn distribution will affect Θ. It can be shown that when the only interaction is between NN's, Θ is governed by the average number $\bar{z}_{\mathrm{Mn}}$ of Mn spins which are NN's of a given Mn spin. For a random Mn distribution, $\bar{z}_{\mathrm{Mn}}=zx$ and Θ is given by Eq. (17). If the Mn distribution is not random, then $\bar{z}_{\mathrm{Mn}}\neq zx$, so that Eq. (17) does not hold.

Equation (15) gives the asymptotic high-T behavior of χ_{Mn}. In practice, the measurements are made at finite T, and some analysis is necessary in order to obtain the asymptotic values of C and Θ. This will be discussed in connection with the interpretation of the data.

III. EXPERIMENTAL TECHNIQUES

A. Samples

Crystals of $Zn_{1-x}Mn_xTe$ were grown by the traveling solvent method, using tellurium as the solvent. The growth temperature was about 900 °C, and the growth rate was about 3 mm/d. The crystals were 11 mm in diameter and 15 mm long. Details of the growth procedure will be published elsewhere.[37] In the present experiments we used two samples with dimensions of $3\times3\times6$ mm. They were cut from crystals with different compositions. Inspection of the samples with a low-power microscope revealed the existence of several grain boundaries in each sample. Atomic absorption analysis[38] gave a Mn concentration $x=0.031$ for one sample and $x=0.040$ for the other. The quoted uncertainty in these values was less than 0.001.

The above values for x represent the average Mn concentrations for the two samples. The variation Δx of x along the length of a given sample was investigated by performing susceptibility and atomic absorption measurements on slices which were cut from that sample. For the sample with $x=0.031$, a change $\Delta x/x\cong0.16$ between the two ends of the sample was found. For the second sample, $\Delta x/x=0.02$. The appreciable gradient for the first sample should not have a significant effect on the interpretation of the data, i.e., the average properties of the sample should correspond closely to those of the average concentration.

B. Magnetometers

Three magnetometers were used in the present work. Susceptibility measurements in the range 4—350 K and $H<50$ kOe were made with a S.H.E Corporation VTS-905 SQUID (superconducting quantum-interference device) magnetometer. The expected accuracy for the magnetic moment was 1%. The accuracy of the temperature measurements with this instrument was evaluated in an independent study,[39] and the results were incorporated into the error analysis of the data.

High-field magnetization data, up to 210 kOe, were made with a very-low-frequency vibrating-sample magnetometer (VLFVSM),[40] operating in a Bitter magnet. These measurements were made with the samples immersed in liquid ^{4}He. The VLFVSM gives a signal which is proportional to the magnetization M. The proportionality constant was determined by comparing the VLFVSM signal at 4.27 K and 48.0 kOe with the value of M at the same temperature and field as obtained from the S.H.E. Corporation SQUID magnetometer. This normalization procedure was applied to each sample.

Magnetization measurements in fields up to 85 kOe were also made at 1.3 and 4.2 K with a vibrating-sample magnetometer (VSM).[41] A NbTi superconducting magnet was used. The data were normalized by using a nickel standard. The estimated accuracy for M in this case was better than 2%.

IV. MAGNETIZATION STEP AT HIGH FIELDS

A. Results and curve fitting

Results for the magnetization of the two samples in fields up to 210 kOe are shown in Figs. 2 and 3. These data were taken with the VLFVSM. The magnetization step near 150 kOe is interpreted as the first step due to level crossings for NN pairs. This interpretation is supported by the analysis below, and by the values of Θ in Sec. VI.

To analyze the data in Figs. 2 and 3 we assume that the magnetization M is the sum of the first magnetization step M_1, as given by Eq. (12), and a background magnetization M_b which is not associated with level crossings,

$$M=M_1+M_b \ . \tag{19}$$

The background magnetization contains two contributions. The first, which is due to the Mn spins in the ab-

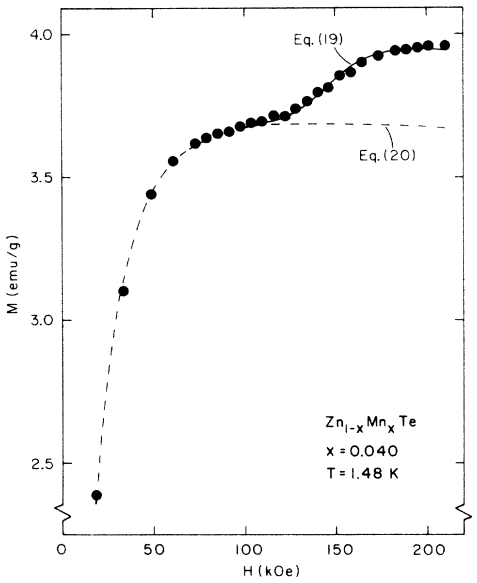

FIG. 2. Magnetization M for $x=0.040$ as a function of magnetic field H. The dashed curve represents Eq. (20) with M_s and T_0 determined from a fit to the data below 86 kOe. The solid curve represents Eq. (19) with M_b as given by the dashed curve and with M_1 as given by a fit of $M-M_b$ to Eq. (12).

sence of level crossings, is approximated by Eq. (3). The second is the diamagnetic contribution of the lattice, $\chi_d H$. Thus,

$$M_b = M_s B_{5/2}(5\mu_B H/k_B(T+T_0)) + \chi_d H \ . \tag{20}$$

For the present samples, $\chi_d = -3.0\times 10^{-7}$ emu/g (Sec. VI), so that the term $\chi_d H$ is small compared to the term which involves the Brillouin function. At high magnetic fields the Brillouin function approaches saturation, and

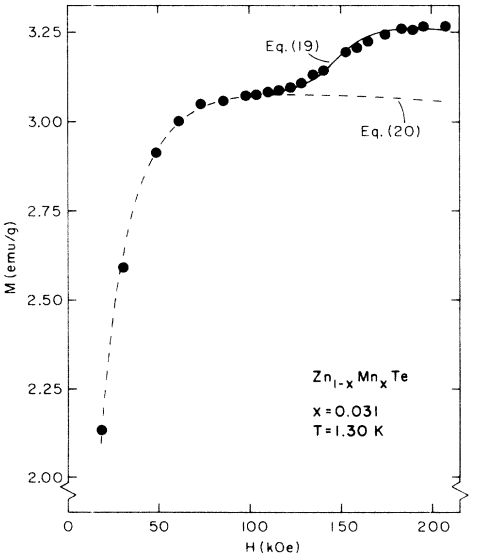

FIG. 3. Magnetization M for $x=0.031$ as a function of H. The dashed curve is the best fit to Eq. (20) using data below 98 kOe. The solid curve represents Eq. (19) with M_b as given by the dashed curve and with M_1 as given by the best fit to Eq. (12).

the diamagnetic term leads to a very slow decrease of M_b with increasing H.

In the first stage of the analysis, the parameters M_s and T_0 are obtained by fitting the magnetization data in fields well below the step to Eq. (20). Using these parameters the background magnetization in fields near the step is calculated and then subtracted from the measured magnetization. The remainder is then fitted to Eq. (12).

For the sample with $x=0.040$ (Fig. 2), a fit of the data below 86 kOe to Eq. (20) gives $M_s=3.739\pm0.013$ emu/g and $T_0=2.105\pm0.055$ K. (These values do not change significantly if the fit is restricted to fields below 80 or 74 kOe.) The background magnetization using these parameters is shown in Fig. 2 as a dashed curve. A fit of $M-M_b$ to Eq. (12) then gives $\delta M=0.274$ emu/g and $H_1=147.2$ kOe. The solid curve in Fig. 2 represents the total magnetization as calculated from Eq. (19) using these parameters and Eqs. (12) and (20).

The uncertainties in H_1 and δM as obtained from the last fit are only 0.7% and 1.8%, respectively. However, a more realistic assessment of the actual uncertainties must include possible errors due to the procedure of subtracting the background M_b. Although the representation of M_b by Eq. (20) is expected to be reasonably accurate, it is not perfect (see Heiman *et al.*, Ref. 26). If we assume an uncertainty of up to 0.03 emu/g in the background magnetization near the step (which we believe to be realistic), the uncertainty in H_1 changes to 3.9% and the uncertainty in δM changes to 10%. Thus, $H_1=147.2\pm5.7$ kOe and $\delta M=0.274\pm0.027$ emu/g. Henceforth we will include the effect of the uncertainty in M_b in all quoted values.

Equation (12), which was used in the preceding analysis, assumes that the width of the magnetization step is solely due to thermal broadening. To account for other possible broadening mechanisms in a phenomenological manner, an alternative analysis was made in which the temperature T in Eq. (12) was replaced by an effective temperature $T_{\rm eff}$. That is,

$$M_1 = \frac{\delta M}{1+\exp[g\mu_B(H_r-H)/k_B T_{\rm eff}]} \ . \tag{21}$$

A fit of $M-M_b$ in Fig. 2 to Eq. (21) gave $T_{\rm eff}=1.96$ K, as compared to $T=1.48$ K. The values for H_1 and δM were 149.3 ± 3.5 kOe and 0.288 ± 0.042 emu/g, respectively.

Applying the same procedures to the data for $x=0.031$ (Fig. 3), the following results are obtained. The parameters for the background magnetization are $M_s=3.120\pm0.013$ emu/g and $T_0=1.911\pm0.064$ K. From the fit of $M-M_b$ to Eq. (12), $H_1=147.7\pm8$ kOe and $\delta M=0.198\pm0.026$ emu/g. From the fit to Eq. (21), $H_1=150.3\pm4.5$ kOe and $\delta M=0.212\pm0.041$ emu/g. The best fit to Eq. (21) gives $T_{\rm eff}=1.84$ K, compared to the actual temperature $T=1.30$ K.

B. Exchange constant J and probability P_2

The NN exchange constant J is related to H_1 by Eq. (2). For $x=0.040$ the value of H_1 which was obtained using Eq. (12) gives $J/k_B=-9.9\pm0.4$ K. For the same sample the value of H_1 obtained from Eq. (21) gives

$J/k_B = -10.0 \pm 0.2$ K. The corresponding values for the sample with $x = 0.031$ are $J/k_B = -9.9 \pm 0.5$ and -10.1 ± 0.3 K. Combining these results, and taking into account possible effects due to the NNN interaction (Sec. II B 4), our final value is $J/k_B = -10.0 \pm 0.8$ K.

The probability P_2 that a Mn spin is in a NN pair is related to δM by Eq. (10). For $x = 0.040$ the value of δM which was obtained from Eq. (12) gives $P_2 = 0.236 \pm 0.024$. Here, the calculated value $M_0 = 5.801$ emu/g for this Mn concentration was used. For the same sample the value of δM which was obtained from Eq. (21) gives $P_2 = 0.248 \pm 0.036$. These experimental values for P_2 agree with the probability $P_2(\text{random}) = 0.230$, which is calculated from Eq. (11) on the assumption that the Mn ions are randomly distributed.

For the sample with $x = 0.031$ the values of δM which were obtained from Eqs. (12) and (21) give $P_2 = 0.220 \pm 0.029$ and 0.236 ± 0.046, respectively. Here, the calculated value $M_0 = 4.493$ emu/g was used. The experimental values for P_2 agree with $P_2(\text{random}) = 0.211$.

V. TECHNICAL SATURATION

In this section we compare experimental results for M_s/M_0 with Eqs. (7) and (8). Results for the technical saturation value M_s were given in the preceding section. These were obtained with a VLFVSM. Independent results for the same samples were obtained from the data in Fig. 4, which were taken with a VSM. For $x = 0.040$ a fit of the VSM data to Eq. (20) gives $M_s = 3.706 \pm 0.022$ emu/g and $T_0 = 1.915 \pm 0.076$ K. For $x = 0.031$, $M_s = 3.100 \pm 0.016$ emu/g and $T_0 = 1.583 \pm 0.063$ K. The rms deviations from the best fits are 0.05 emu/g for $x = 0.040$ and 0.04 emu/g for $x = 0.031$.[42,43]

For both samples the values of M_s which were obtained from the VSM data near 1.3 K agree to better than 1% with those obtained from the VLFVSM data. However, the VSM values for T_0 are slightly lower. The latter discrepancy is attributed to the different field ranges which were used in the fits to the VSM and VLFVSM data; the VSM data start at $H = 0$, whereas the lowest point obtained with the VLFVSM is at 18 kOe. If the fits of the VSM data are restricted to fields above 18 kOe, then (1) the disagreement between the VSM and VLFVSM values for T_0 is reduced to less than 0.09 K, which is within the combined experimental uncertainty, (2) the values of M_s change by only 1%, and (3) the rms deviations between the data and the best fits are reduced by a factor of 3.

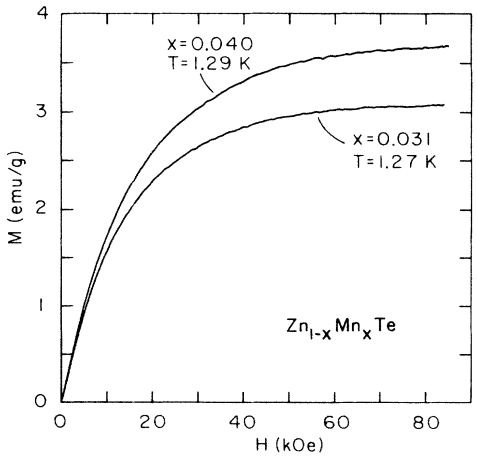

FIG. 4. Magnetization curves for the two samples.

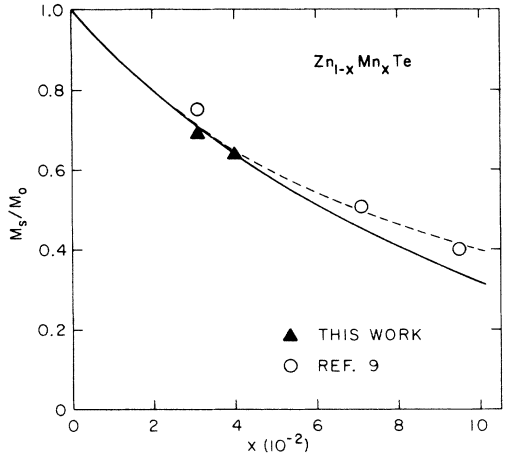

FIG. 5. Ratio M_s/M_0 as a function of x for $Zn_{1-x}Mn_xTe$. The solid and dashed curves represent Eqs. (7) and (8), respectively, with the probabilities P_c calculated assuming a random Mn distribution.

Both the VSM and the VLFVSM results give $M_s/M_0 = 0.64$ for $x = 0.40$ and $M_s/M_0 = 0.69$ for $x = 0.031$. These values are shown in Fig. 5. Also shown are the experimental results of Twardowski *et al.*,[9] at their lowest temperature. The solid curve in Fig. 5 represents Eq. (7), with the probabilities P_c calculated on the assumption that the Mn ions are randomly distributed. This theoretical curve neglects the contribution of clusters with $n_c \geq 4$. The dashed curve represents Eq. (8), which includes the contribution of these large clusters. Note that the solid and dashed curves contain no adjustable parameters. For the smaller x in Fig. 5, both Eqs. (7) and (8) describe the experimental results quite well. However, for the larger x, Eq. (8) gives a better agreement with experiment. This is expected because the percentage of spins which are in clusters with $n_c \geq 4$ increases with increasing x.

VI. LOW-FIELD SUSCEPTIBILITY

A. Results

The low-field susceptibility was measured with a SQUID magnetometer. The data at each temperature were taken using at least two magnetic fields. All fields were small, i.e., in the range $5\mu_B H/k_B T < 0.14$. In such fields the ratio M/H is expected to agree to within 0.2% with the zero-field susceptibility χ. The data for $T > 100$ K, for example, were taken at 10 and 40 kOe. The results in different fields were in good agreement.

The contribution χ_{Mn} of the Mn spins to the zero-field susceptibility was obtained by subtracting the lattice susceptibility χ_d from χ. To determine χ_d we measured the susceptibility of a pure ZnTe crystal. The results were

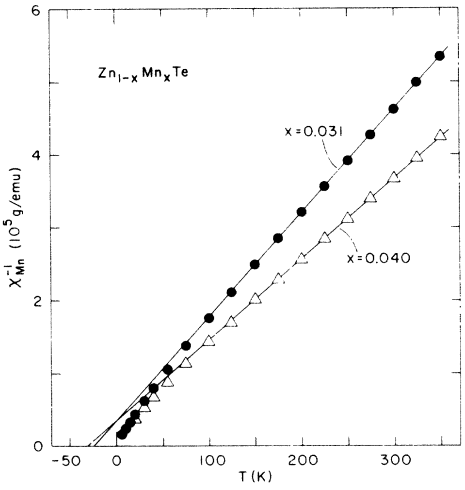

FIG. 6. Temperature dependence of the inverse of the low-field susceptibility χ_{Mn} due to the Mn spins. The straight lines are best fits to Eq. (22) for $T \geq 175$ K.

$\chi_d = -3.02\times10^{-7}$ emu/g at 350 K, -3.02×10^{-7} emu/g at 250 K, and -2.98×10^{-7} emu/g at 10 K. These values are approximately 15% lower than the one quoted in Ref. 44. We therefore performed additional measurements on another pure ZnTe crystal, obtained from another source. The results $\chi_d = -3.01\times10^{-7}$ emu/g at 250 K and -2.98×10^{-7} emu/g at 10 K were in excellent agreement with those obtained for the first crystal. In applying the correction due to the lattice susceptibility, the slight temperature dependence of χ_d can be ignored. In our analysis we used the high-temperature value $\chi_d = -3.02\times10^{-7}$ emu/g throughout. At 350 K the correction due to χ_d amounts to 16% of χ for $x=0.031$ and to 13% of χ for $x=0.040$.

The results for χ_{Mn}^{-1} as a function of T are shown in Fig. 6. The high-temperature portion of each set of data was fitted to the equation

$$\chi_{Mn}^{-1} = (T-\Theta^*)/C^* \ . \tag{22}$$

Here, C^* and Θ^* are effective values for the Curie constant and Curie-Weiss temperature, which depend on the temperature range over which the fit is made. These effective values should be distinguished from the true values of C and Θ, which apply only in the high-temperature limit. The straight lines in Fig. 6 represent the best fits for the range $175 \leq T \leq 350$ K. The parameters for these fits are

$$C^* = (9.019\pm0.028)\times10^{-4} \text{ emu K/g}$$

and

$$\Theta^* = -31.02\pm0.92 \text{ K}$$

for $x=0.040$, and

$$C^* = (7.017\pm0.021)\times10^{-4} \text{ emu K/g}$$

and

$$\Theta^* = -24.54\pm0.86 \text{ K}$$

for $x=0.031$. Additional fits were also made to data in the ranges 150–350, 200–350, and 150–300 K. The results for C^* and Θ^* were close to those quoted above, and they were all included in the determination of C and Θ in the limit of high T.

B. Curie constant and Curie-Weiss temperature

To obtain C and Θ from C^* and Θ^* we used high-temperature-series expansions for a material with randomly substituted magnetic ions. For a fcc magnetic lattice and $S=\frac{5}{2}$, and assuming NN interaction only, a series up to order $(J/k_BT)^6$ is available.[36] This series was used to obtain numerical results for the susceptibility as a function of k_BT/J. The results for different ranges of k_BT/J were then fitted to Eq. (22), which led to values of C^* and Θ^* for each range. By comparing these values to C and Θ, as given by Eqs. (16) and (17), the correction factors C/C^* and Θ/Θ^* were obtained. Using our previous result $J/k_B = -10$ K, the correction factors for different temperature ranges in the present experiments were determined.

The errors which resulted from the use of a truncated series, up to order $(J/k_BT)^6$ only, were estimated in two ways. First, the calculations of C/C^* and Θ/Θ^* were repeated by using shorter series, up to order $(J/k_BT)^4$ or $(J/k_BT)^5$. Second, the known longer series for $S=\infty$ (Ref. 45) was used to evaluate the changes which result from adding three additional terms, up to order $(J/k_BT)^9$. These estimates showed that the truncation errors were small in the present case.

As concrete examples we quote the calculated corrections for the range $175 \leq T \leq 350$ K. For $x=0.031$, $\Theta/\Theta^* = 1.06\pm0.01$ and $C/C^* = 1.004\pm0.001$. For $x=0.040$, $\Theta/\Theta^* = 1.056\pm0.016$ and $C/C^* = 1.005\pm0.002$. Thus, the correction for the Curie constant is less than 1% and the correction for Θ is several percent.

Using the results of the fits to Eq. (22), and the correction factors, the following value are obtained. For $x=0.031$,

$$C = (7.05\pm0.15)\times10^{-4} \text{ emu K/g}$$

and

$$\Theta = -26\pm3 \text{ K} \ .$$

For $x=0.040$,

$$C = (9.1\pm0.2)\times10^{-4} \text{ emu K/g}$$

and

$$\Theta = -33\pm4 \text{ K} \ .$$

The quoted uncertainties include estimates of possible small errors in the temperature and susceptibility data of the SQUID magnetometer (Sec. III). The experimental results for C are in excellent agreement with values calculated using $S=\frac{5}{2}$, $g=2$, and the known Mn concentrations. The calculated values are $C=7.04\times10^{-4}$ emuK/g for $x=0.031$ and 9.09×10^{-4} emu K/g for $x=0.040$.

From the values of Θ and Eq. (17) one obtains $J/k_B \cong -12$ K. This estimate for the NN exchange con-

stant hinges on the assumption of a random Mn distribution and on the neglect of all interactions other than between nearest neighbors. The value $J/k_B \cong -12$ K is in satisfactory agreement with the more accurate result $J/k_B = -10.0 \pm 0.8$ K, which was obtained more directly from the magnetization step. This agreement is an additional confirmation that the magnetization step is due to the first level crossing for NN pairs.

VII. CONCLUSIONS

The present work provides the following strong evidence that the Mn ions are randomly distributed: (1) The probability P_2 which is obtained from the magnitude of the magnetization step agrees with P_2(random). (2) The ratio M_s/M_0 agrees with calculations which assume a random Mn distribution. (3) The exchange constant J which is obtained from the magnetization step is consistent with that which is obtained from Θ assuming a random Mn distribution.

Our experimental values for the Curie constant indicate that $S = \frac{5}{2}$ for each Mn ion. This result differs from that reported earlier.[8,17]

The value $J/k_B = -10$ K which was obtained here for $Zn_{1-x}Mn_xTe$ is approximately 30% larger than the one found in $Cd_{1-x}Mn_xTe$ (Ref. 7), which agrees with the conclusion of McAlister *et al.*[8] and with a recent prediction.[23] Our value for J in $Zn_{1-x}Mn_xTe$ is slightly higher than that obtained recently from neutron scattering;[46] the difference is just outside the combined experimental uncertainty of 10%.

ACKNOWLEDGMENTS

We are grateful to Professor P. A. Wolff for interest and encouragement and to Dr. R. L. Aggarwal for useful discussions. The Francis Bitter National Magnet Laboratory is supported by the National Science Foundation under Contract No. DMR-82-11416. Support for P. Becla was provided by the Office of Naval Research under Contract No. N00014-83-K-0454. Support For D. N. Domingues was provided by the Brazilian Conselho Nacional de Desenvolvimento Científico e Tecnológico (CNPq).

[1]J. K. Furdyna, J. Appl. Phys. **53**, 7637 (1982).

[2]For an example of an early work, see M. M. Kreitman, F. J. Milford, R. P. Kenan, and J. G. Daunt, Phys. Rev. **144**, 367 (1966).

[3]R. R. Galazka, in *Physics of Narrow Gap Semiconductors*, Vol. 152 of *Lecture Notes in Physics*, edited by E. Gornik, H. Heinrich, and L. Palmestshofer (Springer, Berlin, 1982), p. 294.

[4]S. Oseroff and P. H. Keesom (unpublished).

[5]Y. Shapira, S. Foner, D. H. Ridgley, K. Dwight, and A. Wold, Phys. Rev. B **30**, 4021 (1984).

[6]R. L. Aggarwal, S. N. Jasperson, Y. Shapira, S. Foner, T. Skakibara, T. Goto, N. Miura, K. Dwight, and A. Wold, in *Proceedings of the 17th International Conference on the Physics of Semiconductors, San Francisco, 1984*, edited by J. D. Chadi and W. A. Harrison (Springer, New York, 1985), p. 1419.

[7]R. L. Aggarwal, S. N. Jasperson, P. Becla, and R. R. Galazka, Phys. Rev. B **33**, 5132 (1985).

[8]S. P. McAlister, J. K. Furdyna, and W. Giriat, Phys. Rev. B **29**, 1310 (1984).

[9]A. Twardowski, P. Swiderski, M. von Ortenberg, and R. Pauthenet, Solid State Commun. **50**, 509 (1984).

[10]J. Lambe and C. Kikuchi, Phys. Rev. **119**, 1256 (1960).

[11]B. C. Cavenett, Proc. Phys. Soc. London **84**, 1 (1964).

[12]H. H. Woodbury and G. W. Ludwig, Bull. Am. Phys. Soc. **6**, 118 (1961).

[13]S. B. Oseroff, R. Calvo, W. Giriat, and Z. Fisk, Solid State Commun. **35**, 539 (1980); S. B. Oseroff, Phys. Rev. B **25**, 6584 (1982).

[14]A. K. Ramdas, J. Appl. Phys. **53**, 7649 (1982).

[15]D. Heiman, Y. Shapira, and S. Foner, Solid State Commun. **51**, 603 (1984).

[16]J. Spałek, A. Lewicki, Z. Tarnawski, Z. Obuszko, and R. R. Galazka, (unpublished).

[17]In Ref. 8 deviations from $S = \frac{5}{2}$ are reported for two $Zn_{1-x}Mn_xTe$ samples. However, the high-temperature data for one of these samples (sample B in Fig. 6 of this reference) are actually fairly close to those expected when $S = \frac{5}{2}$ and $g = 2$. Only the data for sample A deviate from the expected behavior. The effective moment P which enters into the Curie constant is $2[S(S+1)]^{1/2}\mu_B = 5.9\mu_B$, and not $5\mu_B$ as stated in Ref. 8.

[18]W. H. Brumage, C. R. Yarger, and C. C. Lin, Phys. Rev. **133**, A765 (1961).

[19]W. Y. Ching and D. L. Huber, Phys. Rev. B **30**, 179 (1984). Note that their definition of J differs from ours by a factor of 2.

[20]T. M. Giebultowicz, J. J. Rhyne, W. Y. Ching, and D. L. Huber, J. Appl. Phys. **57**, 3415 (1985).

[21]M. Escorne and A. Mauger, Phys. Rev. B **25**, 4674 (1982).

[22]A. B. Davydov, L. M. Noskova, B. B. Ponikarov, and L. A. Ugodnikova, Fiz. Tekh. Poluprovodn. **14**, 1461 (1980) [Sov. Phys.—Semicond. **14**, 869 (1980)].

[23]B. E. Larson, K. C. Hass, H. Ehrenreich and A. E. Carlsson, Solid State Commun. **56**, 347 (1985).

[24]S. Nagata, R. R. Galazka, D. P. Mullin, H. Akbarzadeh, G. D. Khattak, J. K. Furdyna, and P. H. Keesom. Phys. Rev. B **22**, 3331 (1980).

[25]R. R. Galazka, S. Nagata, and P. H. Keesom, Phys. Rev. B **22**, 3344 (1980).

[26]J. A. Gaj, R. Planel, and G. Fishman, Solid State Commun. **29**, 435 (1979). See also D. Heiman, Y. Shapira, S. Foner, B. Khazai, R. Kershaw, K. Dwight, and A. Wold, Phys. Rev. B **29**, 5634 (1984); A. Twardowski, P. Swiderski, M. von Ortenberg, and R. Pauthenet, Solid State Commun. **50**, 509 (1984); D. Heiman, Y. Shapira, and S. Foner, *ibid.* **51**, 603 (1984).

[27]Typically, T_0 increases with x, but is still smaller than 4 K when $x = 0.1$. Thus, for $T < 2$ K and $H = 100$ kOe the deviation of M from M_s is less than 5% for $x = 0.1$, and is still smaller for lower x.

[28]R. E. Behringer, J. Chem. Phys. **29**, 537 (1958).

[29]M. M. Kreitman and D. L. Barnett, J. Chem. Phys. **43**, 364 (1965).

[30]J. Owen and E. A. Harris, in *Electron Paramagnetic Resonance*, edited by S. Geschwind (Plenum, New York, 1972).

[31]Strictly, there is another contribution to the observed δM which is not due to NN pairs. It arises from another type of

cluster (with four spins which are all NN's of each other), for which the first few magnetization steps occur at the same fields as those for the pairs. However, it is expected that the probability for the occurrence of such quartets is very small for small x, so that they should have a negligible contribution to the observed magnitude of δM.

[32]R. L. Aggarwal and K. C. Hass (private communication).

[33]At very low temperatures, $k_B T < |J'|$, the steps due to NN pairs which have NNN's might be resolved from the steps due to NN pairs which have no NNN's.

[34]O. Okada, J. Phys. Soc. Jpn. **48**, 391 (1980).

[35]G. S. Rushbrooke and D. J. Morgan, Mol. Phys. **4**, 1 (1961).

[36]D. J. Morgan and G. S. Rushbrooke, Mol. Phys. **4**, 291 (1961).

[37]P. Becla (unpublished).

[38]Northern Analytical Laboratory, Amherst, New Hampshire 03031.

[39]N. F. Oliveira, Jr., R. D. Frankel, and Y. Shapira (unpublished).

[40]S. Foner and E. J. McNiff, Jr., Rev. Sci. Instrum. **39**, 171 (1968).

[41]S. Foner, Rev. Sci. Instrum. **30**, 548 (1959).

[42]In some early works [see, e.g., J. A. Gaj, R. Planel, and G. Fishman, Solid State Commun. **29**, 435 (1979)] the magnetization was fitted to Eq. (3) instead of Eq. (20). That is, the diamagnetic contribution of the lattice was neglected. For the present samples the differences between the values of M_s and T_0 obtained from fits to Eqs. (3) and (20) are not significant. However, for very low x these two equations can lead to quite different values of M_s and T_0. In our view, Eq. (20) is preferable because it gives the correct behavior in the limit $x \rightarrow 0$.

[43]In addition to the results in Fig. 4, magnetization data for both samples were also obtained with the VSM at 4.2 K. Analysis of the 4.2-K data gave values for M_s which were about 3% higher than those obtained from Fig. 4. The values for T_0 were about 0.2 K higher.

[44]V. I. Ivanov-Omskii, B. T. Kolomiets, V. M. Melnik, and V. K. Ogorodnikov, Fiz. Tverd. Tela (Leningrad) **11**, 2563 (1969) [Sov. Phys.—Solid State **11**, 2067 (1970)].

[45]G. S. Rushbrooke, R. A. Muse, R. L. Stephenson, and K. Pirnie, J. Phys. C **5**, 3371 (1972).

[46]L. M. Corliss, J. M. Hastings, S. M. Shapiro, Y. Shapira, and P. Becla this issue, Phys. Rev. B **33**, 608 (1986).